# Spatial patterns in optical parametric oscillators with spherical mirrors: classical and quantum effects

**M. Marte and H. Ritsch**

*Institut für Theoretische Physik, Universität Innsbruck, Technikerstr. 25, A-6020 Innsbruck, Austria.*

*ritsch@hbar.uibk.ac.at.*

**K. I. Petsas, A. Gatti and L. A. Lugiato**

*Dipartimento di Fisica, Università degli Studi di Milano, Via Celoria 16, Milano 20133, Italy.*

*lugiato@mi.infn.it.*

**C. Fabre and D. Leduc**

*Laboratoire Kastler–Brossel, Université Pierre et Marie Curie, 4 place Jussieu, Tour 12–Case 74, 75252 Paris Cedex 05, France.*

*claude.fabre@spectro.jussieu.fr.*

**Abstract:** We investigate the formation of transverse patterns in a doubly resonant degenerate optical parametric oscillator. Extending previous work, we treat the more realistic case of a spherical mirror cavity with a finite–sized input pump field. Using numerical simulations in real space, we determine the conditions on the cavity geometry, pump size and detunings for which pattern formation occurs; we find multistability of different types of optical patterns. Below threshold, we analyze the dependence of the quantum image on the width of the input field, in the near and in the far field.



**OCIS codes:** (190.0190) Nonlinear optics; (270.0270) Quantum optics

## References and links

1. Special issue on $\chi^2$ second order nonlinear optics, from fundamentals to applications, edited by C. Fabre and J.-P. Pocholle, in JEOS B: J. Quantum and Semiclassical Opt. **9**, (2) (1997). Special issue on Optical Parametric Oscillators, in Applied Physics B, May 1998.
2. M.A.M. Marte, H. Ritsch, L. A. Lugiato and C. Fabre, "Simultaneous multimode optical parametric oscillations in a triply resonant cavity," Acta Physica Slovaca **47**, 233 (1997).
3. G. S. Agarwal and S. D. Das Gupta, "Model for mode hopping in optical parametric oscillators," J. Opt. Soc. Am. B **14**, 2174 (1997).
4. C. Schwob, P. F. Cohadon, C. Fabre, M. A. M. Marte, H. Ritsch, A. Gatti and L. A. Lugiato, "Transverse effects and mode couplings in optical parametric oscillators," submitted to Appl. Phys. B, Special Issue on Optical Parametric Oscillators, edited by. J. Mlynek and S. 1Schiller.
5. G.-L. Oppo, M. Brambilla and L. A. Lugiato, "Formation and evolution of roll patterns in optical parametric oscillators," Phys. Rev. A **49**, 2028 (1994).
6. A. Gatti and L.A. Lugiato, "Quantum images and critical fluctuations in the optical parametric oscillator below threshold," Phys. Rev. A **52**, 1675 (1995).
7. A. Gatti, H. Wiedemann, L. A. Lugiato, I. Marzoli, G.-L. Oppo and S. M. Barnett, "Langevin treatment of quantum fluctuations and optical patterns in optical parametric oscillators below threshold," Phys. Rev. A **56**, 877 (1997).

#4471 - $15.00 US Received February 02, 1998; Revised June 16, 1998

8. A. Gatti, L. A. Lugiato, G.-L. Oppo, R. Martin, P. Di Trapani and A. Berzanskis, "From quantum to classical images," Opt. Express **1**, 21 (1997), http://epubs.osa.org/oearchive/source/1968.htm.
9. C. Schwob and C. Fabre, "Squeezing and quantum correlations in multimode optical parametric oscillators," preprint, to be submitted to JEOS B: J. Quantum and Semiclassical Opt.
10. E. Lantz and F. Devaux, "Parametric amplification of images," JEOS B: J. Quantum and Semiclassical Opt. **9**, 279 (1997).
11. M. I. Kolobov and L. A. Lugiato, "Noiseless amplification of optical images," Phys. Rev. A **52**, 4930 (1995).
12. L. A. Lugiato and I. Marzoli, "Quantum spatial correlations in the optical parametric oscillator with spherical mirrors," Phys. Rev. A **52**, 4886 (1995).
13. L. A. Lugiato, S. M. Barnett, A. Gatti, I. Marzoli, G.-L. Oppo and H. Wiedemann, "Quantum Images," J. of Nonlinear Optical Phys. and Materials **5**, 809 (1996).
14. L. A. Lugiato and P. Grangier, "Improving quantum-noise reduction with spatially multimode squeezed light," J. Opt. Soc. Am. B **14**, 225 (1997).
15. W. H. Press, B. P. Flannery, S. A. Teukolsky, W. T. Vetterling, *Numerical Recipes; the art of scientific computing*, Cambridge University Press, Cambridge (1986).
16. M. SanMiguel and R. Toral, *Instabilities and Nonequlibrium structures, VI*, Kluwer Academic Pub. (1997).
17. L. A. Lugiato, C. Oldano, C. Fabre, E. Giacobino and R. J. Horowicz, "Bistability, self-pulsing snd chaos in optical parametric oscillators," Il Nuovo Cimento **10** D, 959 (1988).
18. K. I. Petsas, A. Gatti and L. A. Lugiato, "Quantum images in optical parametric oscillators with spherical mirrors and gaussian pump," submitted to JEOS B: J. Quantum and Semiclassical Opt.
19. L. A. Lugiato, A. Gatti, H. Ritsch, I. Marzoli and G.-L. Oppo, "Quantum images in nonlinear optics," J. Mod. Opt. **44**, 1899 (1997).
20. I. Marzoli, A. Gatti and L. A. Lugiato, "Spatial quantum signatures in parametric down-conversion," Phys. Rev. Lett. **78**, 2092 (1997).

## 1. Introduction

Nowadays the optical parametric oscillator (OPO) has become a device with a broad range of applications [1]. The standard descriptions of the OPO are based on a small number of modes for the involved fields, which are characterized by their carrier frequency. In the standard configuration one uses a single mode for each of the involved fields (pump, signal and idler fields), which are coupled by some effective nonlinear coupling constant. All the other modes in the cavity are usually neglected, as they are assumed to be far off resonance or not coupled by the dynamics. In general this assumption is not valid and several transverse or longitudinal mode pairs may contribute to the dynamics. Recently models involving several modes have been developed [2-4]. In some cases a large number of modes contribute, leading to new dynamical phenomena. For the case of a resonator with planar mirrors, it has been demonstrated [5] that in general one has a multimode situation with spatial instabilities leading to the spontaneous formation of various types of transverse optical patterns. Interestingly, below threshold these patterns are somehow still present, but hidden in the correlations of the quantum noise (quantum images [6,7,8]).

In recent papers [2,4] we have shown that when using a resonator with nonplanar mirrors and a finite–sized pump field, a new nonlinear coupling between different signal and idler mode pairs exists. This introduces a strikingly different physical behaviour of the system and leads to new and interesting phenomena such as the combined oscillation of various modes above threshold with fixed relative phases. Even multistability between different such solutions can be obtained and the squeezing properties of the emitted light are modified [9]. In contrast to this treatment, which is restricted to a small number of effectively contributing modes, we will consider here the case of quasidegenerate cavity configuration with very small transverse mode splitting. In this limit a very large number of coupled modes participate in the dynamics. This strongly influences the

#4471 - $15.00 US Received February 02, 1998; Revised June 16, 1998

pattern formation, both above threshold on a classical level and below threshold on a quantum level.

Apart from the possibility to have a prototype of a well–controlled, easy accessible and variable nonlinear dynamical system, there might also be some practical applications in image processing, storage and amplification [10,11] or ultrafast optical (de-)multiplexing. Let us finally remark that the basic structure of the underlying mathematical equations is very similiar to the Gross-Pitajewski equation governing the (almost zero-temperature) dynamics of a Bose-condensate in an external trap, where similiar features might be observable.

In this paper we analyze the case of a degenerate OPO with spherical mirrors and finite–size input beams. On a classical level, we analyze pattern formation above threshold, and show under which conditions some of the results of [5] extend to the case of spherical mirrors. On a quantum level, we consider the case of the OPO below threshold and study the variation of the quantum images in the near [12] and in the far [13] field, when the width of the input beam is gradually reduced.

## 2. Model

Let us consider a cavity with spherical mirrors and a *thin* nonlinear $\chi^{(2)}$-crystal with an effective nonlinear coupling strength $\chi$. The cavity is coherently pumped by an input field $E_p$ at a frequency $\omega_p$ from the outside and the single input/output mirror is assumed highly reflective at the pump frequency as well as at the signal frequency $\omega_s = \omega_p/2$. We consider the doubly resonant case of an OPO with a common cavity for the two fields, which have a common Rayleigh length $z_r$. For the overall geometry we restrict ourselves to a quasi–planar or a quasi–confocal geometry. In this case, the effective transverse mode spacing $\xi$ is on the order of, or even less than, the cavity linewidths $\kappa_s$ and $\kappa_p$ for the signal and pump field, respectively, and many transverse modes can contribute to the dynamics [4]. We will concentrate on the classical aspects of the field dynamics first. Eliminating the longitudinal dependence by using the paraxial and the mean field approximations, we find the following equations for the transverse dynamics of the slowly varying pump field amplitude $A_p(r,\phi,t)$ and the signal field $A_s(r,\phi,t)$ [7]:

$$\frac{\partial}{\partial t}A_p(r,\phi,t) = -(\kappa_p + i\delta_p - i\xi L_p)A_p(r,\phi,t) - \frac{\chi}{2}A_s^2(r,\phi,t) + E_p(r,\phi) + W_p(t), \quad (1)$$

$$\frac{\partial}{\partial t}A_s(r,\phi,t) = -(\kappa_s + i\delta_s - i\xi L_s)A_s(r,\phi,t) + \chi A_p(r,\phi,t)A_s^*(r,\phi,t) + W_s(t), \quad (2)$$

where the transverse variables $r$ and $\phi$ denote the distance from the axis of the system and the angular variable, respectively. The effect of diffraction and spherical mirrors is contained in the differential operator [12]:

$$L_k = \frac{w_k^2}{4}\nabla_T^2 - \frac{r^2}{w_k^2} + 1. \quad (3)$$

Here $\delta_k = \omega_k^{00} - \omega_k$ ($k \in \{p,s\}$) is the detuning between the chosen carrier frequency of the fields and the eigenfrequency of the $TEM_{00}$-mode closest to resonance. $E_p(r,\phi)$ represents an externally applied pump amplitude and $w_k = \sqrt{(2z_r c)/\omega_k}$ is the minimum waist of the intracavity fields. The additive noise terms $W_k$ have been introduced to model fluctuations of the pump field or other noise sources. On one hand such noise are helpful to speed up the convergence of the numerical solutions; on the other hand, for a proper choice of the time-correlation functions of $W_p$ and $W_s$ Eqs. (1,2) are Langevin equations which govern the dynamics of the system on a quantum level, in the Wigner representation [7]. Without such noise sources, we have a trivial solution of these equations given by $A_s = 0$, $A_p = E_p/(\kappa_p + i\delta_p)$. This solution is stable only below threshold.

#4471 - $15.00 US Received February 02, 1998; Revised June 16, 1998

One notices that the eigenfunctions of each operator $L_k$ are just the usual transverse Gauss-Laguerre functions. Inserting the corresponding mode expansions for all fields leads to the standard coupled mode equations [4]. Unfortunately, any analytical treatment of these equations seems impossible at present. Let us, however, emphasize here that for the ideal degenerate confocal cavity, *i.e.* for $\xi = 0$, the spatial differential operator disappears from the above equations and we get independent OPO's at each spatial point. Such a system has quite intriguing physical properties, as e.g. localized squeezing [14]. Note that on the other hand, in the limit in which a quasi–planar cavity becomes an ideal planar cavity one has that $\xi \to 0$ but, simultaneously, $w_k \to \infty$ in such a way that $\xi w_k^2$ converges to a finite value, so that the effects of $\nabla_T^2$ (diffraction in the paraxial approximation) do not vanish.

The case of finite mirror size can be treated by confining the action of the operators $L_k$ to the mirror surface, and by avoiding periodic boundary conditions. Although in practice one usually works in a regime where the mirror boundaries seem to play no essential role, the spontaneous formation of optical patterns with broken rotational symmetry could be very sensitive to even small boundary effects.

We will solve Eqs. (1,2) by numerical integration starting from zero for all three fields, using a combination of a split-step and a modified mid-point method [15]. Special care has to be taken concerning the noise part [7] as e.g. outlined in a recent work by M. San Miguel and R. Toral [16]. In order to test the integration procedure, we have used various boundary shapes (round, square) and sizes, as well as different noise intensities, grid sizes and time steps to check that the physical properties are independent of the numerical details of calculation.

## 3. Spatial patterns in a doubly resonant degenerate quasi–confocal OPO

We assume that the pump field has a simple Gaussian configuration with width $w_e$, *i.e.* $E_p(r,\phi) = E_0 \exp\left(-r^2/w_e^2\right)$. In addition, we will assume a quasi-confocal cavity setup, which implies inversion symmetry $A_k(r,\phi) = A_k(r,\phi+\pi)$ [or alternatively $A_k(r,\phi) = -A_k(r,\phi+\pi)$] of all intracavity fields; this cuts the number of points needed for the numerical solution in half.

Depending on the pump–size, pump–strength, detunings and on the effective transverse mode spacing (including the crystal) we find a great diversity in the physical behaviour of the system. Varying the mode spacing (e.g. by changing the cavity geometry), we can control the number of effectively participating modes in the dynamics from a nearly single mode case if $\xi \gg \kappa_s$ to a large number of contributing modes for $\xi \ll \kappa_s$. By varying the detunings we can choose the modes out of the transverse manifold which are dominantly excited. Similarly, by changing the shape (e.g. the size) of the pump field we can select which modes are effectively excited. In addition, via the pump–*size* we can also control the nonlinear intermode coupling [2,4] from independent excitation (large pump $w_e \gg w_p$) to a strong mode coupling ($w_e \approx w_s$). Finally, we can influence the dynamics by changing the pump *strength*.

Let us first consider the simple case of a perfect confocal cavity, where $\xi = 0$. One easily finds that for points $(r,\phi)$ where the pump intensity is large enough so that $|E_p(r,\phi)|^2 > \left(\kappa_p^2+\delta_p^2\right)\left(\kappa_s^2+\delta_s^2\right)/\chi^2$, the OPO is above threshold. For instance, for $\delta_s = \delta_p = 0$ and by choosing $E_p$ real, one has in steady-state:

$$A_p(r,\phi) = \frac{\kappa_s}{\chi},\; A_s^2(r,\phi) = \frac{2}{\chi}\left[E_p(r,\phi) - \frac{\kappa_p\kappa_s}{\chi}\right]. \tag{4}$$

The intracavity pump field is clamped to a fixed value, and the intracavity signal field intensity at the location of the nonlinear crystal reproduces the variation of the pump field amplitude, reduced by a fixed quantity.

#4471 - $15.00 US Received February 02, 1998; Revised June 16, 1998

In contrast, for points where $|E_p(r,\phi)|^2 < \left(\kappa_p^2 + \delta_p^2\right)\left(\kappa_s^2 + \delta_s^2\right)/\chi^2$, the OPO is below threshold. For $\delta_s = \delta_p = 0$ and $E_p$ real one has, e.g.:

$$A_p(r,\phi) = \frac{E_p(r,\phi)}{\kappa_p},\ A_s(r,\phi) = 0. \tag{5}$$

For a Gaussian pump, one therefore finds there exists a circular area around the origin inside which the signal beam has the shape of the central part of Gaussian, and outside which the signal field is zero, whereas the intracavity pump field intensity has the shape of the outer part of a Gaussian outside the circle, and has a flat top inside the circle.

When $\xi \neq 0$, the treshold has to be determined numerically. In the following, we will focus on a number of selected examples. In all calculations of this section we have $\chi = 0.1\kappa_s$ and $\kappa_p = 3\kappa_s$. For such values, the plane wave threshold for a planar cavity corresponds to $E_p = 30\kappa_s$ for $\delta_s = \delta_p = 0$.

For $\xi \gg \kappa_s$, the results are qualitatively similar to those of the two-mode treatment of the degenerate OPO. For a nonzero detuning of pump and signal fields, situations arise that display spatially oscillating patterns, which might be related to the self-pulsing found in [17]. The rotational symmetry is still preserved.

### *3.1 Resonant multimode case*

We proceed directly to a more complex situation and consider a small ($\xi \approx \kappa_s$), or even very small ($\xi \ll \kappa_s$) transverse mode spacing. As we can see from Eqs. (1,2), this decreases the influence of diffraction, which mediates spatial cross-coupling, and leads eventually to individual spatial points oscillating independently. Let us for the moment assume $\delta_p = \delta_s = 0$, the corresponding stationary signal field intensity distribution is shown in Fig. 1.

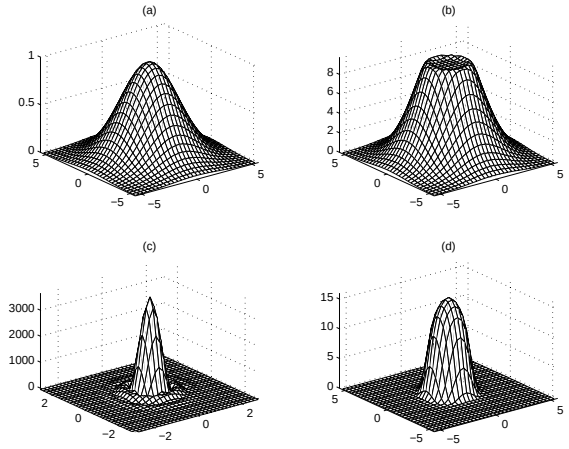


Figure 1. Modulus of steady-state field amplitude as a function of the transverse position: (a) input field, (b) intracavity pump field, (c) signal far field and (d) signal intracavity field for $\delta_p = \delta_s = 0$, $w_e = 3w_p$, $\xi = 0.05\kappa_s$ and $E_p = 42\kappa_s$. In the near field plots the length scale is $w_p$; in the far field diagram it is $z\lambda_s/(2\pi w_p)$, where $z$ is the distance from the cavity.

For a small transverse mode spacing $\xi = 0.05\kappa_s$, we see that inside a central region, where the pump field is locally above threshold, the intracavity pump field is clamped by the dynamics to its threshold value, yielding a flat top. This behaviour is therefore very close to the one encountered in the perfect confocal configuration. In the outside region, where the pump is below threshold, the intracavity pump field is merely

#4471 - $15.00 US
Received February 02, 1998; Revised June 16, 1998

proportional to the input. This behaviour gets more pronounced for smaller $\xi$ and larger $w_e$, where more and more modes contribute to the intracavity fields. The signal field is strongly confined to the above threshold region, where its shape roughly corresponds to the input pump field. Outside this region it is almost zero. The strong directional confinement of the far field shows the transverse phase coherence of the total signal field, which is still present despite the weak cross-coupling.

### *3.2 Detuned multimode operation: transverse patterns*

In this section we discuss the most complex situation and allow for multimode operation as well as a detuning of the signal carrier field with respect to the corresponding $TEM_{00}$ mode. As it is known this leads to spatial instabilities and optical pattern formation [5] in the case of flat mirrors and plane wave input field.

Let us first look at the case of a $TEM_{00}$ input field. Many modes are excited and we have a fairly strong cross-coupling between the different modes. This leads to a fixed relative phase operation of several modes, yielding various rather smooth spatial distributions, which can in some sense be interpreted as an effective oscillating mode. This notion is, however, somewhat artificial as the effective mode depends on the pump strength and pump shape. An example is shown in Fig. 2, where we plot the stationary intracavity pump and signal fields for a small transverse mode spacing.

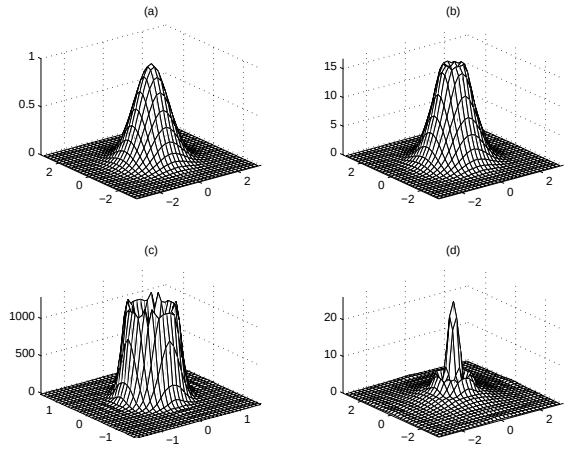


Figure 2. Same as in Fig. 1 except for $w_e = w_p$, $\xi = 0.2\kappa_s$, $\delta_s = -2.5\kappa_s$, $E_p = 65\kappa_s$: (a) input field, (b) intracavity pump field, (c) signal far field and (d) signal intracavity field.

The signal far field exhibits a ring-shaped distribution, which closely reminds the below threshold results found in [7], while the near field configuration is Bessel-like. Only in the case of a very small mode coupling $\xi = 0.075\kappa_s$, we find a pattern with broken rotational symmetry, similar to the roll patterns discussed just below.

For a wider input pump field ($w_e \gg w_p$) again many modes are possibly excited, but the relative phase coupling is less strong and there is more room for dynamical adjustment of the fields. This allows for breaking rotational symmetry and for the spontaneous dynamical formation of various optical patterns. The situation is richer than in the plane wave case. In the following we will show this on some specific examples.

Close to threshold one finds a roll (stripe) pattern as shown in Fig. 3, where we have small mode coupling, broad resonant pump and negative signal detuning.

#4471 - $15.00 US Received February 02, 1998; Revised June 16, 1998

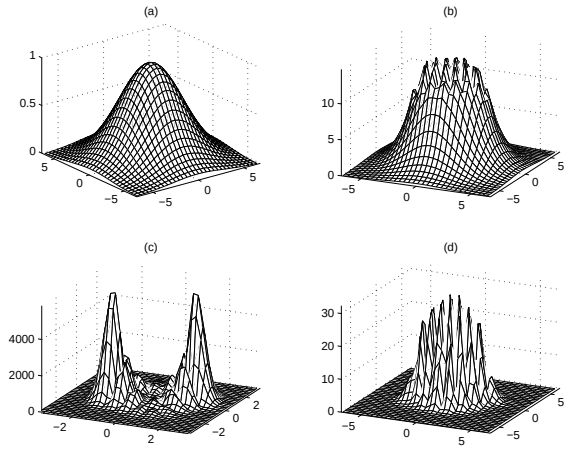


Figure 3. Same as in Fig. 2 but for $w_e = 4w_p$, $\xi = 0.25\kappa_s$, $\delta_s = -1.5\kappa_s$: (a) input field, (b) intracavity pump field, (c) signal far field and (d) signal intracavity field.

Once such stripes in some direction have formed, they only very slowly change their direction, driven by the input noise. However, comparing many different runs, starting each time at zero field with a small amount of "white" noise the stripes are randomly oriented, but show a well defined modulation length depending on $\delta_s$ and $E_p$. In some rare cases a ring shape pattern appears. Once such a pattern has formed, it seems to be stable against the formation of stripes even for a fairly large amount of noise and for slow changes of the system parameters. As one might expect, the stripe pattern leads to a two-peaked intensity distribution in the far field.

For an increased pump strength other types of patterns appear. Roughly at 1.75 times threshold, spiral shaped patterns form frequently, as shown in Fig. 4. Once formed they show a slow rotation, *i.e.* the end of the arms grow. Again, these turn out to be quite stable against noise and slow changes of the system parameters. The rotation speed depends on $E_p$ and $w_p$ and is much slower than the other time scales in the system. For these parameter ranges stripes and spirals are stable at the same time. Even seeding a stripe pattern into the input for an existing spiral has no effect, as the modification of the pump field induced by the spiral prevents gain for the seeded stripes, and vice versa. Hence there is multistability of various patterns induced *via* the backaction of the existing pattern on the pump field.

Figure 4. The movie shows the formation of a spiral pattern for the same values of the parameters as in Fig. 3 but for $E_0 = 70\kappa_s$.

Even further above threshold new patterns, cointaining a number of point–like structures, appear. Typical examples in the near field are shown in Fig. 5.

#4471 - $15.00 US Received February 02, 1998; Revised June 16, 1998

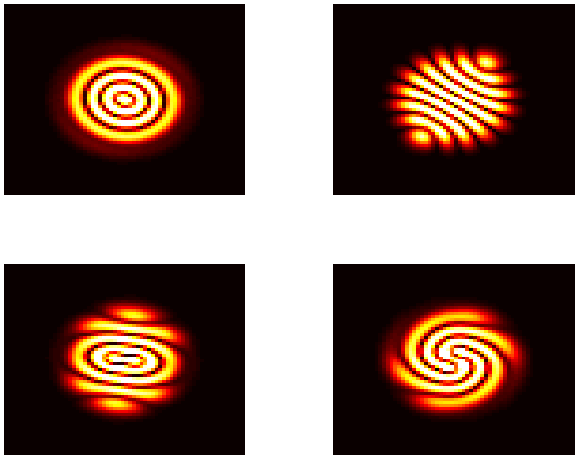

Figure 5. Various quasi–stationary patterns found for the signal field for $w_e = 4w_p$, $\xi = 0.25\kappa_s$, $\delta_p = 0$, $\delta_s = -1.5\kappa_s$ and $E_0 = 85\kappa_s$.

In all this, the shape of the mirror seems to have little influence; it is the finiteness and size of the pump, which plays the most important role.

## 4. Quantum images below threshold

In this section we consider a quasi–planar cavity, instead of quasi–confocal. Below threshold, and not too close to threshold, the pump depletion can be neglected. If moreover, as in [12], [13] we assume that the pump field is not reflected at all by the cavity mirrors, the quantity $A_p$ in Eq. (2) can be expressed as a given function of $r$, $\phi$ equal to the input field $E_{in}$. Hence, Eq. (2) becomes self-contained for the signal field $A_s(r, \phi, t)$, and Eq. (1) can be dropped altogether.

If we consider any circle $\mathcal{C}$ centered on the system axis, at steady-state below threshold, any observable $\mathcal{O}(r, \phi, t)$ is uniform on average over the circle because of the cylindrical symmetry and is constant in time. However, if we consider the spatial correlation function at steady-state $F(r, \Delta\phi, t) = \langle \mathcal{O}(r, \phi, t)\, \mathcal{O}(r, \phi', 0) \rangle$ where $r$ is the radius of circle $\mathcal{C}$, we obtain a function of $\Delta\phi = \phi - \phi'$ which exhibits a spatial modulation. This structure, visible in the spatial correlation function, has been called "*quantum image*" [6,12]. The same is true for the spectrum associated with the correlation

$$\widetilde{F}(r, \Delta\phi, \omega) = \int_{-\infty}^{+\infty} dt\; e^{-i\omega t} F(r, \Delta\phi, t)\,. \tag{6}$$

As in [12,13], we will consider as observable a quadrature of the signal field, $\mathcal{O} = A_s \exp(-i\varphi_L) + A_s^* \exp(i\varphi_L)$, for an appropriate phase $\varphi_L$ of the local oscillator field used to detect the quadrature. While in [12,13] the input field was a plane wave, we assume here that it corresponds to a gaussian profile of width $w_e$, and analyze how the result changes when we decrease gradually $w_e$ from infinity (plane wave case) to values on the order of $w_s$. In particular, we want to see whether the main phenomena identified in [12,13] persist, or are washed out by the finite size of the pump.

The calculation of the correlation function is carried out with the help of an expansion of the signal field in terms of Gauss-Laguerre modes [12,13]. In the present case, however, the finiteness of $w_e$ couples the modes [2,4]; a complete description of the calculation will be given in a future paper [18]. Figures 6 and 7 show the spectral density $\widetilde{F}(r, \Delta\phi, \omega)$ [normalized to $\widetilde{F}(r, \Delta\phi = 0, \omega)$] for $\omega = 0$. In the near field [*i.e.* in Figs. 6(a) and 7(a)] we take $r = w_s$ and $\varphi_L = 0$. In the far field [Figs. 6(b) and 7(b)], on

#4471 - $15.00 US
Received February 02, 1998; Revised June 16, 1998

the other hand, we evaluate the correlation function at a distance $z = 20z_r$ from cavity center, and we take $r = w_s \left[1 + (z/z_r)^2\right]^{1/2}$ and [19]

$$\varphi_L = \frac{r^2}{w_s^2 \left[1 + \left(\frac{z}{z_r}\right)^2\right]} \frac{z}{z_r} - (q_c + 1) \tan^{-1}\left(\frac{z}{z_r}\right) + \frac{\pi}{2}, \tag{7}$$

where $q_c$ is the order of a frequency-degenerate family of Gauss-Laguerre modes which is exactly resonant with the signal frequency $\omega_s$ [12] and $q = 2p + l$, where $p$ and $l$ are the radial and angular indices of the Gauss-Laguerre functions, respectively. In both figures 6 and 7 we have $q_c = 3$. The value of the input field is measured as a dimensioneless parameter $\overline{E}_{in} = E_{in}\chi/\kappa_s$; in the plane wave limit $w_e \to \infty$, the threshold value is $\overline{E}_{in} = 1$.

When the OPO is below but close to threshold the main feature is the presence of a regular modulation in the correlation as a function of $\Delta\phi$. For the value of $\overline{E}_{in}$ considered in Fig. 6, the system is 10% below threshold in the plane wave limit $w_e \to \infty$. As shown in [12] for $w_e = \infty$, when approaching the threshold the contribution of the resonant family becomes dominant and, because the circle $\mathcal{C}$ is chosen in such a way that the modes $p = 1$, $l = 1$ vanish, the correlation function $\widetilde{F}(r, \Delta\phi, \omega = 0) / \widetilde{F}(r, \Delta\phi = 0, \omega = 0)$ arises only from the contribution of the two modes $p = 0$, $l = 3$, so that getting close to threshold the curve approaches the function $\cos(3\Delta\phi)$, as shown by the red line in Fig. 6(a). Reducing $w_e$, the modulation becomes less regular and less pronounced, but it is still quite remarkable for $w_e = 1.4w_s$. It must be taken into account, in addition, that decreasing $w_e$ the threshold value for $\overline{E}_{in}$ increases.

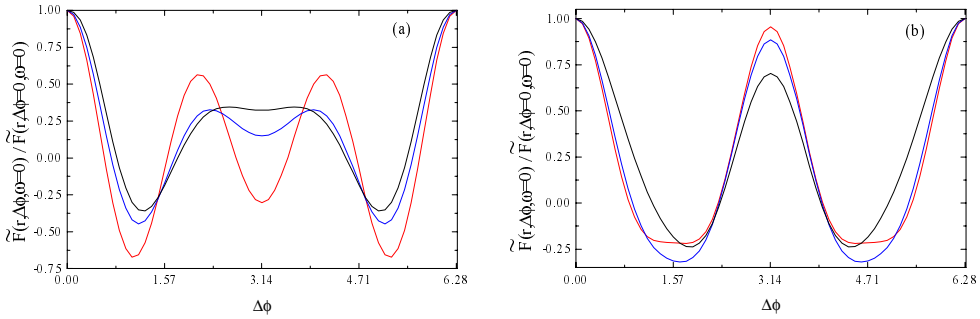


Figure 6. The correlation function $F(r, \Delta\phi, \omega)$ divided by $F(r, \Delta\phi, \omega = 0)$ is plotted as a function of $\Delta\phi$ for a quadrature component with the phase $\phi_L$ specified in the text. We fix $\omega = 0$ and the value of $r$ as described in the text. We set $\overline{E}_{in} = 0.9$, $\xi = 0.5\kappa_s$, and $\delta_s = -1.5\kappa_s$. (a) Near field, (b) Far field. Red curve: $w_e \to \infty$, blue curve: $w_e = 2.8w_s$, black curve: $w_e = 1.4w_s$.

#4471 - $15.00 US
Received February 02, 1998; Revised June 16, 1998

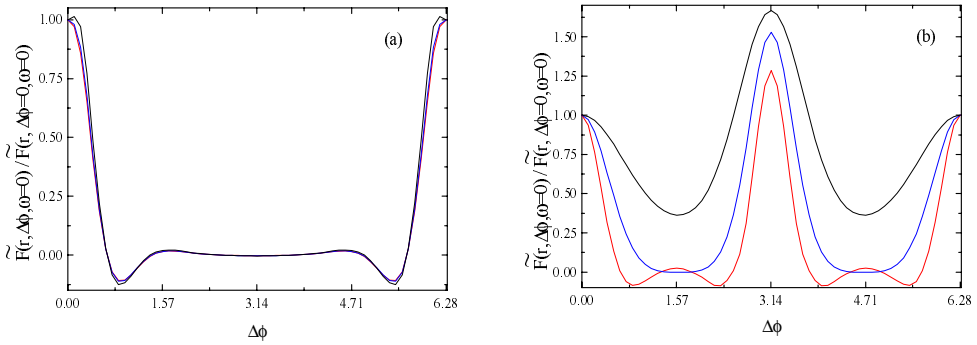


Figure 7. Same as in Fig. 6, but for $\overline{E}_{in} = 0.6$, $\xi = 0.1\kappa_s$, and $\delta_s = -0.3\kappa_s$.

On the other hand, well below threshold the interesting feature arises in the far field [13]. Precisely, as shown by Fig. 7(b), there is a peak for $\Delta\phi = \pi$ higher than the peak in $\Delta\phi = 0$. As shown in [19,20] this is a purely quantum effect which provides evidence from a spatial viewpoint of the twin photon emission in the OPO. Figure 7 shows that this feature (which becomes more and more pronounced as $\xi$ is decreased) is quite robust with respect to the reduction of $w_e$, up to when $w_e$ becomes on the order of $w_s$. The correlation as a function of $\Delta\phi$ becomes broader as $w_e$ is decreased.

**Acknowledgements**

This research was carried out in the framework of Network QSTRUCT ("*Quantum Structures*") of the TMR program of the EU, and supported by the Austrian Science Foundation FWF Project No. S6506. M. M. was supported by an *APART* fellowship of the Austrian Academy of Sciences.